

See discussions, stats, and author profiles for this publication at: <https://www.researchgate.net/publication/6983210>

# Electronic Properties of Capped, Finite-Length Armchair Carbon Nanotubes in an Electric Field

ARTICLE *in* THE JOURNAL OF PHYSICAL CHEMISTRY B · JULY 2006

Impact Factor: 3.3 · DOI: 10.1021/jp056724k · Source: PubMed

---

CITATIONS

8

---

READS

25

4 AUTHORS, INCLUDING:



**Chuan Chen**

MeiHo University

16 PUBLICATIONS 47 CITATIONS

SEE PROFILE



**Chia-Chang Tsai**

Hermes Microvision Inc.

25 PUBLICATIONS 328 CITATIONS

SEE PROFILE



**Jian-Ming Lu**

National Applied Research Laboratories

36 PUBLICATIONS 288 CITATIONS

SEE PROFILE

## Electronic Properties of Capped, Finite-Length Armchair Carbon Nanotubes in an Electric Field

Chuan Chen,<sup>‡,§</sup> Chia-Chang Tsai,<sup>†</sup> Jian-Ming Lu,<sup>†,§</sup> and Chi-Chuan Hwang<sup>\*,†</sup>

Department of Engineering Science, National Cheng Kung University, 701 Tainan, Taiwan, Department of Information Science, Meiho Institute of Technology, 912 Pingtung, Taiwan, and National Center for High-Performance Computing, No. 28, Nanke 3rd Road, Sinshih Township, Tainan County 744, Taiwan

Received: November 20, 2005; In Final Form: March 31, 2006

This study investigates the electronic properties of finite-length armchair carbon nanotubes in an electric field (**E**) using a single- $\pi$ -band tight-binding model. Three different tip configurations are considered, namely, open ends with hydrogen terminations (H-terminations), one end capped with half of C<sub>60</sub> fullerene and the other end open with H-terminations, and both ends capped with half of C<sub>60</sub> fullerene. In general, the electronic states and energy gaps of low-energy electronic structures are highly sensitive to changes in the direction and magnitude of the applied electric field and to the tip configuration. The present results show that the electric field induces a strong modulation of the state energies and energy gaps of the current nanotubes, changes their energy spacings, and prompts the occurrence of semiconductor–metal transitions (SMTs). It is found that the SMTs occur more frequently as the direction of the electric field approaches the symmetry axis or when its magnitude becomes sufficiently large. The present results also indicate that the Fermi levels and energy gaps of the three nanotubes considered in this study are strongly influenced by the cap configuration. Finally, the convergent decay behavior of the energy gap which is observed as the length of the nanotube is increased is also strongly dependent on the tip configuration.

Since their original discovery in 1991 by Iijima,<sup>1</sup> the unique electronic structures of carbon nanotubes have attracted intensive experimental<sup>2–6</sup> and theoretical<sup>7–12</sup> study. The single-walled carbon nanotube (SWNT) has been the subject of particular interest since this one-dimensional quantum wire possesses either metallic, semiconductive, or semimetallic properties depending on its diameter and chirality.<sup>12</sup> Conventionally, the geometric structure of SWNTs is indicated by a pair of integer indices ( $m,n$ ) relating to the wrapping superlattice vector, where  $0 \leq n \leq m$ . The geometric features of the SWNT structure are reflected directly in the physical properties of the nanotube, i.e., in its electronic, magnetic, and transport properties, and in its optical excitation characteristics. SWNTs are employed for a diverse range of applications, including scanning probes,<sup>13</sup> actuators,<sup>14</sup> nanoelectronic devices,<sup>15–17</sup> and electron field emission sources.<sup>18</sup> Previous studies have shown that the tip shape of a SWNT has a fundamental influence on its field emission properties.<sup>19,20</sup> For example, a thin nanotube with a closed cap produces a highly stable emission pattern. However, a nanotube with an open end generates an indistinct emission pattern. Therefore, it is desirable to study the fundamental properties of carbon nanotubes with different end closures in order to develop a more comprehensive understanding of their field emission properties.

It has been reported that the electronic structures of infinite-length carbon nanotubes are strongly affected by the presence of a uniform electric field (**E**<sub>⊥</sub>) oriented perpendicular to the nanotube axis.<sup>21–23</sup> The electric field modifies the low-energy

electronic states of the nanotube and hence modulates the energy gaps. The carbon nanotubes prepared in laboratories are of a finite size. For example, the scanning tunneling microscope (STM) technique has been utilized to produce carbon nanotubes with a finite length of  $\sim 100$  Å.<sup>24</sup> Finite size effects in carbon nanotubes have been intensively studied.<sup>25–30</sup> However, the effects of the tip configuration on the electronic structure of the nanotube under an electric field are less well understood. Accordingly, the objective of the present study is to investigate the effects of an electric field on the electronic properties of finite-length armchair carbon nanotubes with different end cap configurations.

This study considers (5,5) armchair carbon nanotubes with three different cap configurations, as described below. Using the tight-binding approximation, the  $\pi$ -electronic states of the (5,5) armchair SWNTs are calculated in accordance with the nearest-neighbor tight-binding model. The effect of the carbon nanotube curvature on the coupling between the  $\sigma$ - and  $\pi$ -electrons is known to be very small and is therefore neglected in the present calculations.<sup>31</sup> In a (5,5) armchair nanotube, the ideal end closure is that of half of C<sub>60</sub> fullerene. This study considers three different tip configuration types (or boundary conditions), namely: type I, both ends open with hydrogen terminations (H-terminations); type II, one end with half of C<sub>60</sub> fullerene and the other end open with H-terminations; type III, both ends with half of C<sub>60</sub> fullerene. In the present simulations, the C–C bond length is assumed to be  $a_{C-C} \cong 1.42$  Å and nanotubes of increasing length are modeled simply by increasing the number of sections ( $N$ ) along the tube axis. Note that each section contains 10 carbon atoms for a (5,5) carbon nanotube. Therefore, the total number of carbon atoms ( $N_C$ ) in the type I, type II, and type III armchair SWNTs is given by  $10N$ ,  $10N + 30$ , and  $10N + 60$ , respectively. The distance between each

\* Corresponding author. E-mail: chchwang@mail.ncku.edu.tw. Tel: (+886)-6-2757575 ext. 63348. Fax: (+886)-6-2766549.

<sup>†</sup> National Cheng Kung University.

<sup>‡</sup> Meiho Institute of Technology.

<sup>§</sup> National Center for High-Performance Computing.

section ( $L$ ) is  $L \cong 1.23 \text{ \AA}$ . The Hermitian Hamiltonian matrix is built from the subspace spanned by the  $N_C$  wave functions of  $2p_z$  orbitals. In the presence of an electric field, the nearest-neighbor Hamiltonian is given by

$$H = \sum_i \epsilon_i(\mathbf{E}) c_i^\dagger c_i + \sum_{i,j} (-\gamma_0) c_i^\dagger c_j$$

where  $\epsilon_i(\mathbf{E})$  is the unperturbed on-site potential induced by the electric field,  $\gamma_0 = 3.033 \text{ eV}$  is the nearest-neighbor hopping integral, and  $\{c_i^\dagger, c_j\}$  are creation and annihilation operators. In performing the current computations, it is convenient to use rectangular coordinates and to represent the atom position by  $(x_i, y_i, z_i)$ , where  $i = 1, 2, 3, \dots, N_C$ . Note that the origin of this coordinate system is located at the center of the nanotube cylinder. The distance between the  $i$ th carbon atom and the  $j$ th carbon atom is given by

$$\Delta_{ij} = \sqrt{\Delta x^2 + \Delta y^2 + \Delta z^2}$$

where  $\Delta x = |x_i - x_j|$ ,  $\Delta y = |y_i - y_j|$ , and  $\Delta z = |z_i - z_j|$ . In the absence of  $\mathbf{E}$ , the Hamiltonian matrix elements are given by

$$H_{ij} = \begin{cases} -\gamma_0 & \text{if } a_{C-C} - \delta \leq \Delta_{ij} \leq a_{C-C} + \delta \\ 0 & \text{if others} \end{cases}$$

where  $\delta = 0.05 \text{ \AA}$ .

When armchair carbon nanotubes are subjected to an electric field, their on-site energy is changed. In this study, the electric field is assumed to be of the form  $\mathbf{E} = E \cos \alpha_E \hat{z} + E \sin \alpha_E \hat{x} = \mathbf{E}_{||} + \mathbf{E}_{\perp}$ , where  $\alpha_E$  is the angle between  $\mathbf{E}$  and the symmetry axis ( $\hat{z}$ ). Note that  $E$  has units of  $\gamma_0/\text{\AA}$ . Under the influence of the electric field, the diagonal elements of the Hamiltonian matrix are changed from zero to

$$H_{ii} = -E \cos \alpha_E z_i - E \sin \alpha_E x_i$$

The electronic state energies of finite-length carbon nanotubes, which can be obtained by diagonalizing the  $N_C \times N_C$  Hamiltonian matrix, are expressed as  $E^{c,v}(M, \mathbf{E})$ , where  $M (=1, 2, 3, \dots, N_C)$  represents the discrete state and  $c$  and  $v$  correspond to the unoccupied and occupied states, respectively. Note that an energy gap ( $E_g$ ) may exist between the highest occupied state and the lowest unoccupied state.

This study commences by investigating the electronic structure of the type I carbon nanotube, in which  $N_C = 2000$  and the nanotube length is approximately 24.6 nm. As shown in Figure 1a, in the absence of an electric field, the type I nanotube is a gapless metal. The discrete electronic states are symmetric to the Fermi energy ( $E_F$ ) and are doubly degenerate. However, when the nanotube encounters a uniform electric field, its electronic states are strongly modulated. As  $\mathbf{E}_{||}$  increases, some state energies become larger, while others become smaller. Consequently, state crossings take place, particularly at large values of  $\mathbf{E}_{||}$ . Additionally, the energy gap disappears at certain magnitudes of the electric field. Furthermore, more electronic states are grouped into the low-energy regions. At  $\alpha_E = 90^\circ$ , the electronic structures are barely changed for conditions of  $E < 0.01 \gamma_0/\text{\AA}$  (not shown). The main reason for this is that  $\epsilon_i(\mathbf{E}_{\perp})$  at  $E < 0.01 \gamma_0/\text{\AA}$  is much smaller than the typical hopping integral  $\gamma_0$ . The electronic properties of the nanotube, e.g., the state energy, energy width, energy gap, and wave function, are influenced more strongly at large values of  $\mathbf{E}_{\perp}$ . Furthermore, the effects of  $\mathbf{E}_{||}$  on the electronic properties are much greater than those of  $\mathbf{E}_{\perp}$  since the electric potential difference is large

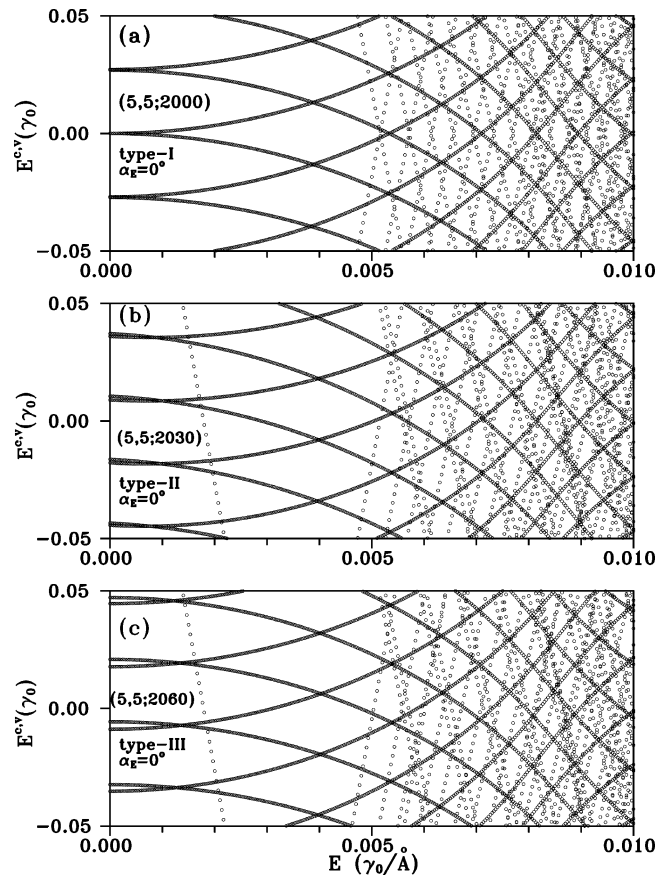


**Figure 1.** Electric-field-dependent low-energy states of (5,5) finite-length carbon nanotube with 200 sections, in which the tip is configured with (a) two H-terminated ends, (b) one end with half of  $C_{60}$  fullerene and the other end with H-terminations, and (c) both ends with half of  $C_{60}$  fullerene at  $\alpha_E = 0^\circ$ .

at the symmetry axis. This result clearly reflects the geometric features of the nanotube, i.e., its length is much larger than its radius.

In the type II carbon nanotube (Figure 1b), the occupied states are not symmetric to the unoccupied states at  $E_{||}$ , and  $E_F$  is changed as a result both of the broken geometric symmetry along the tube axis and the effect of one end of the nanotube being closed by a cap with half of  $C_{60}$  fullerene. Compared to the type I nanotube, the state crossings in the type II nanotube occur at a smaller magnitude of the electric field. Furthermore, the state degeneracy is destroyed as a result of the cap effect. In the type III carbon nanotube, shown in Figure 1c, the existence of two caps with half of  $C_{60}$  fullerene causes similar effects, i.e., the state crossings occur at a lower electric field and the state degeneracy is destroyed. However, the main difference in the electric-field-dependent electronic properties of the type II and type III nanotubes are the changes in  $E_F$  and  $E_g$  at  $\mathbf{E} = 0$ . When the magnitude of  $\mathbf{E}_{||}$  increases, it becomes increasingly difficult to study the evolution of the electron states with the electric field due to the large number of discrete states which are formed.

To better understand the semiconductor–metal transitions (SMTs) in the current nanotubes, this study conducts a systematic investigation into the variation of the energy gap with the direction and magnitude of the electric field. Figure 2a presents the electric-field-dependent energy gap for the type I armchair SWNT at  $E < 0.01 \gamma_0/\text{\AA}$ . At  $\alpha_E = 0^\circ$ , it can be seen that the energy gap is strongly influenced by the electric field (indicated by the light solid curve). SMTs occur as  $\mathbf{E}_{||}$  increases

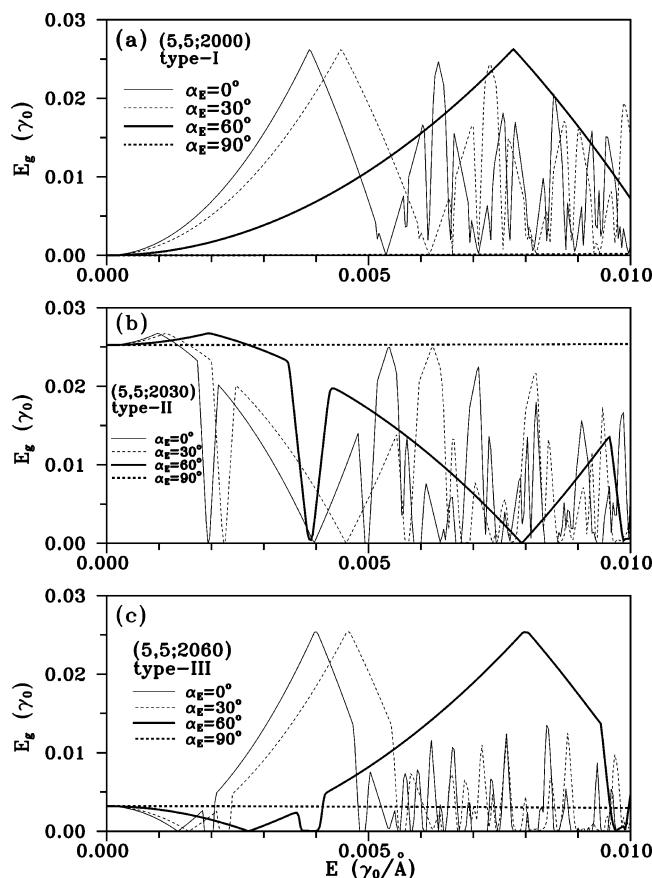


**Figure 2.** Influence of electric field direction on electric-field-dependent energy gaps of (5,5) finite-length carbon nanotube with 200 sections, in which the tip is configured with (a) two H-terminated ends, (b) one end with half of C<sub>60</sub> fullerene and the other end with H-terminations, and (c) both ends with half of C<sub>60</sub> fullerene.

and take place more frequently at electric fields of higher magnitude. However, as the electric field deviates from the symmetry axis, the energy-gap modulation effect becomes weaker. Therefore, at  $\alpha_E = 90^\circ$  (indicated by the heavy dashed curve), it is observed that  $E_g$  is largely unaffected by the electric field. In other words, the type I SWNT remains metallic at small values of  $E_\perp$ . In general, more SMTs take place at larger values of  $E$  and smaller values of  $\alpha_E$ . Similar energy-gap modulations are found in the type II and type III SWNTs, as shown in parts b and c of Figure 2, respectively. The effect of the electric field in type II and type III carbon nanotubes is similar to that in type I carbon nanotubes. However, in the type II SWNT (Figure 2b), the single cap with half of C<sub>60</sub> fullerene induces an energy gap at  $E = 0$  and at  $\alpha_E = 0^\circ$ , and the SMTs occur at a lower value of  $E_\parallel$  than in type I nanotubes. Compared to the type I armchair SWNT, the presence of a single end cap prompts a greater number of SMTs. Figure 2c shows that the type III armchair SWNT has more SMTs than the type II system as a result of its two end caps. In general, the results of Figure 2 confirm that the presence of end caps significantly increases the energy gap modulation. The predicted energy gaps can be verified by performing STM measurements.<sup>5,6,32,33</sup>

This study also investigates the length-dependent energy gaps of the type I, type II, and type III armchair SWNTs. As shown in Figure 3,  $E_g$  decays smoothly with an increasing tube length (i.e., an increasing number of sections). Furthermore, it is observed that tubes with  $3q - 2$ ,  $3q - 1$ , and  $3q$  sections, respectively (where  $q$  is an integer), exhibit different energy gap behaviors with increasing tube length. For the type I

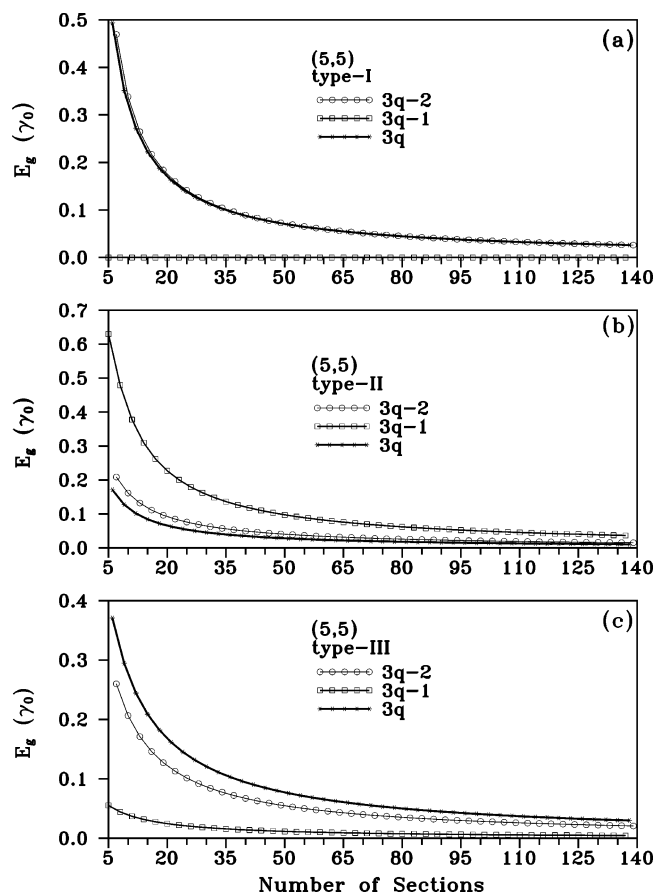


**Figure 3.** Influence of tube length ( $3q - 2$ ,  $3q - 1$ , and  $3q$  sections) on converging decay behavior of energy gaps of (5,5) finite-length carbon nanotubes configured with (a) two H-terminated ends, (b) one end with half of C<sub>60</sub> fullerene and the other end with H-terminations, and (c) both ends with half of C<sub>60</sub> fullerene.

nanotubes (Figure 3a), the value of  $E_g$  for the tubes with  $3q - 2$  and  $3q$  sections, respectively, decreases along the same curve. By contrast, the tube with  $3q - 1$  sections is a gapless metal. For the type II nanotubes (Figure 3b), the tube with  $3q - 1$  sections has a large energy gap, while the tubes with  $3q - 2$  and  $3q$  sections have medium and small energy gaps, respectively. The type III nanotubes exhibit a similar behavior to that of the type II nanotubes, but the value of  $E_g$  is smaller. The tubes with  $3q$  and  $3q - 2$  sections have large and medium energy gaps, respectively, while the tube with  $3q - 1$  sections has a smaller energy gap. In all three nanotube types,  $E_g$  tends toward zero as the tube length approaches infinity. In general, Figure 3 reveals that the magnitude of  $E_g$  is highly sensitive to changes in the tip configuration for SWNTs of finite length.

It has been reported that chirality plays an important role in determining the physical properties of a carbon nanotube.<sup>10–12</sup> However, it is not easy to model the tip structures of finite length carbon nanotubes other than armchair or zigzag CNTs. For (9,0) zigzag carbon nanotubes, and the (5,5) armchair carbon nanotube, the ideal end closure is that of half of C<sub>60</sub> fullerene. As part of this study, the low-energy electric properties of capped (9,0) tubes were investigated for comparison purposes. The results showed that the influence of the electric field on low-energy electronic structures was similar to that reported above for armchair carbon nanotubes.

In summary, this study has investigated the electronic properties of three types of finite-length armchair carbon nanotubes under an electric field. The results have shown that the electronic states and energy gaps are strongly dependent on



the direction and magnitude of the electric field and on the configuration of the nanotube tip. The electric field causes a strong modulation of the energy gap, generates state crossings, yields more low-energy states, and changes the state degeneracy. It has been shown that semiconductor–metal transitions occur more frequently when the electric field is closer to the symmetric axis of the nanotube or when the magnitude of the electric field is sufficiently large. The length-dependent energy gap exhibits a converging decay, which is sensitive to the tip structure. The predicted electronic properties can be verified by STM measurement and provide a valuable understanding of the field emission properties of nanotubes with and without end caps.

**Acknowledgment.** This study was supported in part by the National Science Council of Taiwan, Republic of China, under Grant No. NSC 94-2811-E-006-010.

**Supporting Information Available:** Images of carbon nanotube field emission display arrays and graphs of buckling behavior of double-wall nanotubes vs single-wall nanotubes. This material is available free of charge via the Internet at <http://pubs.acs.org>.

## References and Notes

- Iijima, S. *Nature (London)* **1991**, 354, 56.
- Iijima, S.; Ichihashi, T.; Ando, Y. *Nature (London)* **1992**, 356, 776.
- Carvert, P. *Nature (London)* **1992**, 357, 365.
- Ge, M.; Sattler, K. *Science* **1993**, 260, 515–517.
- Wildoer, J. W. G.; Venema, L. C.; Rinzler, A. G.; Smalley, R. E.; Dekker, C. *Nature (London)* **1998**, 391, 59.
- Ouyang, M.; Huang, J. L.; Cheung, C. L.; Lieber, C. M. *Science* **2001**, 292, 702.
- Mintmire, J. W.; Dunlap, B. I.; White, C. T. *Phys. Rev. Lett.* **1992**, 68, 631.
- Kane, C. L.; Mele, E. J. *Phys. Rev. Lett.* **1997**, 78, 1932.
- Tanaka, K.; Okahara, K.; Okada, M.; Yamabe, T. *Chem. Phys. Lett.* **1992**, 191, 469.
- Ajiki, H.; Ando, T. *J. Phys. Soc. Jpn.* **1996**, 65, 505.
- Shyu, F. L.; Chang, C. P.; Chen, R. B.; Lin, M. F. *J. Phys. Soc. Jpn.* **2003**, 72, 454.
- Saito, R.; Dresselhaus, G.; Dresselhaus, M. S. *Physical Properties of Carbon Nanotubes*; Imperial College Press: London, 1998.
- Dai, H.; Hafner, J. H.; Rinzler, A. G.; Colbert, D. T.; Smalley, R. E. *Nature (London)* **1996**, 384, 147.
- Baughman, R. H.; Cui, C.; Zakhidov, A. A.; Iqbal, Z.; Barisci, J. N.; Spinks, G. M.; Wallace, G. G.; Mazzoldi, A.; Rossi, D. D.; Rinzler, A. G.; Jaschinski, O.; Roth, S.; Kertesz, M. *Science* **1999**, 284, 1340.
- Tans, S. J.; Verschuere, A. R. M.; Dekker, C. *Nature (London)* **1998**, 393, 49.
- Postman, H. W. Ch.; Teepen, T.; Yao, Z.; Grifoni, M.; Dekker, C. *Science* **2001**, 293, 76.
- Matsumoto, K.; Kinoshita, S.; Gotoh, Y.; Kurachi, K.; Kamimura, T.; Maeda, M.; Sakamoto, K.; Kuwahara, M.; Atoda, N.; Awano, Y. *Jpn. J. Appl. Phys.* **2003**, 42, 2415.
- Rinzler, A. G.; Hafner, J. H.; Nikolaev, P.; Lou, L.; Kim, S. G.; Tomanek, D.; Nordlander, P.; Colbert, D. T.; Smalley, R. E. *Science* **1995**, 269, 1550.
- Han, S.; Ihm, J. *Phys. Rev. B* **2000**, 61, 9986.
- Jonge, N. D.; Allieux, M.; Doytcheva, M.; Kaiser, M. *Appl. Phys. Lett.* **2004**, 85, 1607.
- Zhou, X.; Chen, H.; Zhong, O. Y. *J. Phys.: Condens. Matter* **2001**, 13, L635–L640.
- Kim, Y. H.; Chang, K. J. *Phys. Rev. B* **2001**, 64, 153404(1–4).
- O’Keeffe, J.; Wei, C.; Cho, K. *Appl. Phys. Lett.* **2000**, 80, 676.
- Venema, L. C.; Wildoer, J. W. G.; Temminck Tuinstra, H. L. J.; Dekker, C. *Appl. Phys. Lett.* **1997**, 71, 2629.
- Wu, J.; Duan, W.; Gu, B. L. *Appl. Phys. Lett.* **2000**, 77, 2554.
- Zhu, H. Y.; Klein, D. J.; Schmalz, T. G.; Rubio, A.; March, N. H. *J. Phys. Chem. Solids* **1997**, 59, 417.
- Chen, R. B.; Lu, B. J.; Tsai, C. C.; Chang, C. P.; Shyu, F. L.; Lin, M. F. *Carbon* **2004**, 42, 2873.
- Liang, W. L.; Wang, X. J.; Yokoijima, S.; Chen, G. *J. Am. Chem. Soc.* **2000**, 122, 11129.
- Meunier, V.; Senet, P.; Lambin, Ph. *Phys. Rev. B* **1999**, 60, 7792.
- Venema, L. C.; Wildoer, J. W. G.; Janssen, J. W.; Tans, S. J.; Temminck Tuinstra, H. L. J.; Kouwenhoven, L. P.; Dekker, C. *Science* **1999**, 283, 52.
- Benedict, L. X.; Louie, S. G.; Cohen, M. L. *Phys. Rev. B* **1995**, 52, 8541.
- Odom, T. W.; Huang, J. L.; Kim, P.; Lieber, C. M. *Nature (London)* **1998**, 391, 62.
- Kim, P.; Odom, T. W.; Huang, J. L.; Lieber, C. M. *Phys. Rev. Lett.* **1999**, 82, 1225.